Physics and Chemistry of Minerals (2022) 49:19
https://doi.org/10.1007/s00269-022-01197-3

ORIGINAL PAPER

Recent developments on high-pressure single-crystal X-ray diffraction at the Partnership for eXtreme Xtallography (PX2) program

Dongzhou Zhang[1,2] · Jingui Xu[1,2] · Przemyslaw K. Dera[1] · Mark L. Rivers[2] · Peter J. Eng[2] · Vitali B. Prakapenka[2] · Joanne E. Stubbs[2]

Received: 6 January 2022 / Accepted: 27 April 2022

Abstract
Single-crystal X-ray diffraction is an established method to constrain the structure and chemistry of crystalline minerals under high-pressure conditions. Partnership for eXtreme Xtallography (PX2) is a high-pressure crystallographic research program dedicated to diamond anvil cell research. Located at the experimental station 13-BM-C of the Advanced Photon Source, PX2 provides 10 μm-level focused X-rays at a fixed energy of 28.6 keV, a 6-circle heavy duty diffractometer and a state-of-the-art Pilatus3 1 M photon-counting detector, optimized for a variety of advanced crystallography experiments. A suite of auxiliary equipment including a compact multipurpose optical table and remote membrane-based pressure control has been installed to facilitate the experiments. Resistive and laser heating capabilities have been commissioned to provide high-temperature sample environments for the study of the planetary interior. In this manuscript we present a few examples to demonstrate the experimental capabilities at PX2.

Keywords High pressure · High temperature · Crystallography · X-ray diffraction

Introduction

Earth is a very complex and dynamic system and geologic phenomena such as seismicity and volcanism have major impacts on society. Proper understanding of these geological phenomena requires knowledge of the microscopic structure of earth-forming materials and how their physical and chemical properties change at extreme pressure–temperature conditions (Stixrude and Lithgow-Bertelloni 2005; Xu et al. 2008). Crystallographic investigations of minerals at various thermodynamic conditions provide fundamental information about the structural parameters such as density, atom coordination geometry, bond lengths, etc., which govern the physical and chemical properties of minerals and are necessary for building reliable geophysical and geochemical models (Dera et al. 2013; Lavina et al. 2014).

To date, X-ray diffraction is the most popular approach to carry out crystallographic investigations on minerals. There are two main diffraction-based approaches for high P–T in-situ crystallographic studies that differ in sample preparation (Lavina et al. 2014; Prescher and Prakapenka 2015; Shen and Mao 2017). Most equation of state (EoS) studies utilize powder X-ray diffraction (PXD) technique, in which the sample is a finely ground powder containing a multitude of microscopic, randomly oriented crystal grains (typical requirement for satisfactory particle statistics is more than 10^6 grains in the X-ray illuminated spot) (Shen and Mao 2017). On the other side of the spectrum, there is single-crystal X-ray diffraction (SXD), which utilizes one or a few near-perfect single crystal specimens (Dera et al. 2013; Zhang et al. 2017). SXD involves slightly more sophisticated sample preparation and loading, while offering some significant advantages over PXD. Obtaining structural information from PXD using full profile refinement methods such as the Rietveld technique is challenging with high-pressure data, especially for low-symmetry crystals, and the results are often ambiguous. SXD data, on the other hand, directly

This article is part of a Topical Collection "Experimental and Analytical Techniques at Extreme and Ambient Conditions", guest edited by Stella Chariton, Vitali B. Prakapenka and Haozhe (Arthur) Liu.

✉ Dongzhou Zhang
dzhang@hawaii.edu

[1] Hawaii Institute of Geophysics and Planetology, University of Hawaii at Manoa, Honolulu, HI 96822, USA

[2] GeoSoilEnviroCARS, University of Chicago, Argonne, IL 60439, USA

Published online: 22 May 2022

reflects the crystal structures of minerals and can yield much more reliable and detailed structural constraints on mineral behavior, including changes in space group, bond lengths and angles, and polyhedral distortions (Hu et al. 2017; Xu et al. 2018; Yong et al. 2019; Zhang et al. 2016a, b). Such information offers an important step towards achieving an atomic level understanding of the structural controls of the physical and chemical properties that are relevant, for example, in interpretation of seismic data (Hu et al. 2017; Xu et al. 2018).

In-situ SXD has been extensively used for mineral physics research and has significantly contributed to the development of this field. The concepts of comparative crystal chemistry, isostructural surfaces in the pressure–temperature-composition space, crystal-chemical trends, etc. have all been coined and developed largely based on SXD experiments conducted in the 80's and 90's (e.g., Hazen and Finger 1982). These conventional SXD experiments have been done with laboratory X-ray sources and are mostly limited to pressure of about 10 GPa or less. These limitations make extrapolation of the detailed compression mechanism trends obtainable with the SXD approach to actual conditions of the interesting geologic environments quite challenging (Lavina et al. 2014). Moreover, conventional laboratory SXD has been thought to be of limited application to cases of structural phase transitions involving large density discontinuities, especially those proceeding via reconstructive mechanism, because the sample usually turns into a polycrystalline aggregate after the transition. Recent developments in synchrotron-based high-pressure SXD techniques have opened new opportunities to explore the behavior of single crystals with much smaller sizes (down to few micrometers) to significantly higher pressures (above 100 GPa) while retaining the main advantages (level of detail, quality and reliability of crystallographic information, higher quality of EoS data, ability to solve new crystal structures in case of phase transitions) of SXD techniques (Dera et al. 2013; McMahon 2012; Zhang et al. 2017).

Partnership for eXtreme Xtallography (PX2) has been providing experimental capabilities for high-pressure diamond anvil cell research at the GeoSoilEnviroCARS (GSECARS) facility at the Advanced Photon Source (APS) since 2014 (Zhang et al. 2017). The PX2 project is a collaboration between the University of Hawaii and GSECARS and is hosted by GSECARS at experimental station 13-BM-C. This project provides focused X-rays at 28.6 keV and a 6-circle heavy duty diffractometer, optimized for a variety of advanced crystallography experiments including SXD and PXD crystal structure determination, phase relationship investigation, EoS studies and thermal diffuse scattering. Currently, we support simultaneously high pressure–temperature crystallographic experiments using resistive- and laser-heated diamond anvil cells. The beamline has a well-established and very active user base, and there have been more than 30 groups of users worldwide annually.

Beamline instrumentation

X-ray optics and single crystal diffraction setup

The GSECARS bending magnet branch 13-BM receives 6 mrad of horizontal beam fan. A mask close to the shield wall blocks a central 1 mrad section dividing the fan into two separate beams for experimental stations 13-BM-C (1.5 mrad) and 13-BM-D (2.5 mrad) (Shen et al. 2005). The inboard beam for the 13-BM-C station is first bounced down by a vertical Kirkpatrick–Baez (K–B) focusing mirror (Eng et al. 1998), located in the optics station 13-BM-B. To maximize spatial separation of the beams towards 13-BM-C and 13-BM-D, the inboard part of the X-ray fan is deflected by a single-bounce Rowland circle monochromator with an exit angle ranging between 10° and 30°. Because of the single-bounce design, the setup operates at fixed energy, since changes of the 13-BM-C monochromator angle change the beam path in the experimental station. At present PX2 operates at constant energy of 28.6 keV (0.434 Å) using a Si(311) crystal, with a bandwidth of ~ 1 eV (Zhang et al. 2017). The Rowland circle monochromator utilizes an asymmetrically cut and dynamically bent crystal which partially focuses the beam in the horizontal direction. Beam focusing in the vertical direction (and removal of higher-order harmonic contamination) is achieved with a one-meter-long dynamically bent Rh-coated silicon vertical focusing mirror. A 320-mm long second-stage mirror has been installed in the 13-BM-C hutch to form compound horizontal focusing for the X-rays. Once focused, the X-ray spot size at PX2 is ~ 12 µm (H) × 18 µm (V), measured at the full-width-at-half-maximum. A motorized rhenium-based pinhole (50 µm in diameter) is placed ~ 70 mm away from the sample to cut the tails of the focused X-ray.

13-BM-C is equipped with a heavy-duty high-precision Newport six-circle kappa-geometry diffractometer (4 circles for sample rotation + 2 circles for detector rotation, Fig. 1) (Zhang et al. 2017). The Newport diffractometer features include high-speed (up to 15 deg/s), high sample-environment load capacity (up to 25 lb), high precision of rotation (sphere of confusion below 50 µm) and multiple degrees of freedom for sample and detector manipulation, making it an ideal apparatus for the advanced crystallography experiments. The diffractometer is compatible with a wide range of X-ray detectors, and in 2018, we upgraded the 15-year-old MAR165 (Rayonix) CCD X-ray area detector to a state-of-the-art, fast Pilatus3 (Dectris) 1 M X-ray area detector with 1 mm Si sensor. The Pilatus3 1 M detector has the best signal-to-noise ratio and the least background among

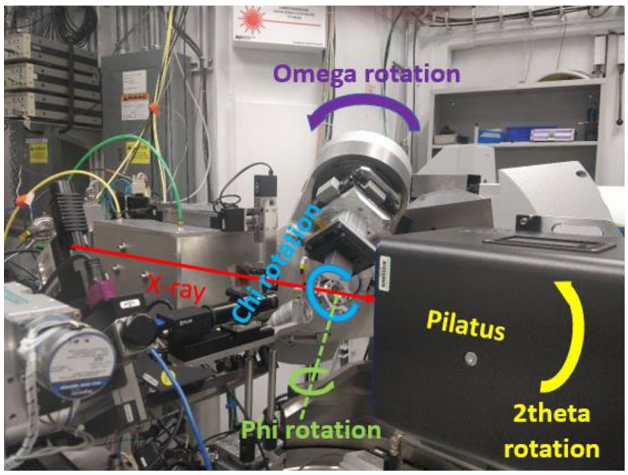

Fig. 1 Diffraction geometry of the 13-BM-C diffractometer. The sample is mounted in a diamond anvil cell and the new Pilatus3 detector is used to collect diffraction patterns. Four of the six rotational axes are shown (Phi, chi and omega for the DAC, and 2theta for the X-ray area detector)

all detectors that have been tested at PX2, and also features good time resolution (25 frames/s, 0.002 s readout time) and a suitable detector area (169 mm × 179 mm), all of which make it ideal for high-pressure experiments at PX2. The Pilatus3 detector can save diffraction images automatically into Crystallographic Binary File (CBF) format, which is a more efficient compressed format compared to the TIF images typically saved by other X-ray area detectors (Bernstein and Hammersley 2006). The advantages of the new Pilatus3 detector over the older MAR165 CCD detector are listed in Table 1. The Pilatus3 significantly reduces the total experimental time and uses less data storage space, making it possible to carry out high-throughput high-pressure diffraction experiments.

The single-crystal diffraction data collection is controlled by the SPEC program (Certified Scientific Software) and has a Python-based user-interface (UI, Fig. 2). The UI provides calibration information for single-crystal diffraction data processing software such as APEX (Bruker) and

Table 1 Comparison of the data collection time and storage efficiency between the old MAR165 CCD and the new Pilatus 1 M detector

Detector	MAR165 CCD	Pilatus3 1 M
Typical measurement condition	70 degrees opening diamond anvil cell and 1 detector position	
Total number of images	70 (step scans) + 7 (wide segments), tiff image	70 (step scans only), cbf image
Experimental time	Typical exposure time: 1 s/° CCD readout time: 2.5 s 70 * (1 s + 2.5 s) + 7 * (10 s + 2.5 s) = 332.5 s	Typical exposure time: 0.5 s/° 70 * 0.5 s = 35 s
Hard drive space	77 * 8196 kB = 631 MB	70 * 1006 kB = 70.4 MB

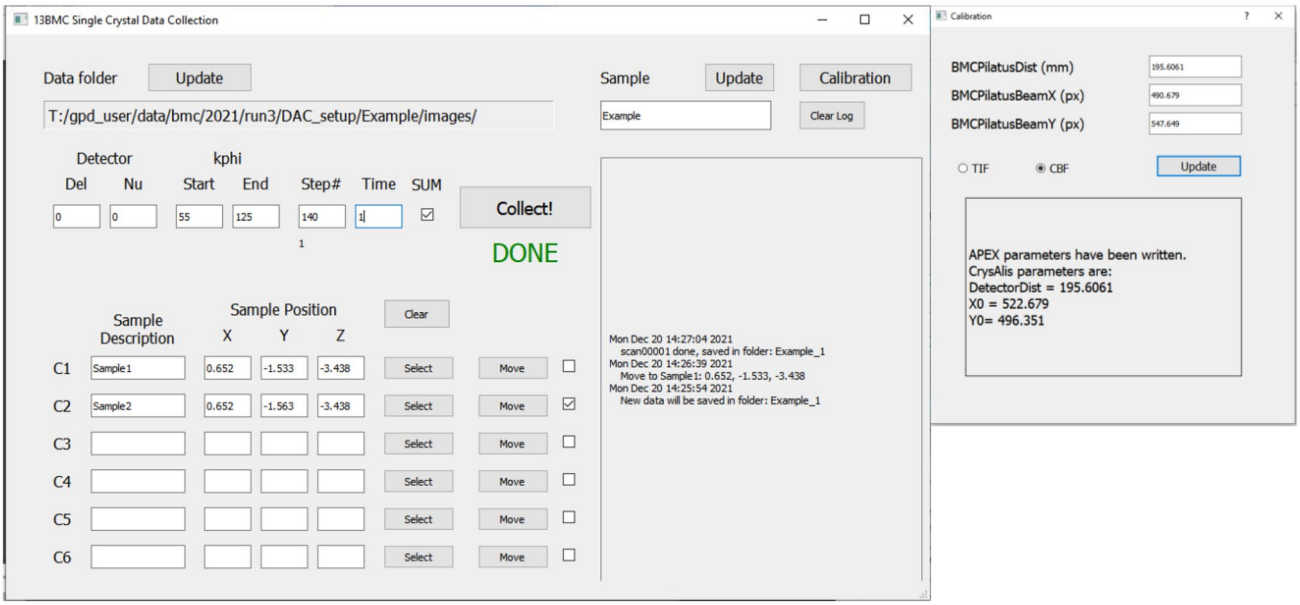

Fig. 2 Screenshot of python-based data collection UI and the calibration panel for the Pilatus3 detector

CrysAlisPro (Rigaku), as well as data collection setups such as sample position, detector position, scanning phi angle range, total number of frames and exposure time per frame. The UI also keeps a log file. The calibration information is automatically written into the metadata of the CBF images and is readable by APEX and CrysAlisPro.

The quality of data produced by a diffraction instrument can be evaluated by the figures of merit of the resulting structural refinements, e.g., R_1, wR_2 and goodness of fit (GooF) (Sheldrick 2008). R_1 and wR_2 both describe the agreement between the modeled and observed crystal structure model. R_1 is weighted by the absolute value of the scattering factor $|F|$ whereas wR_2 is weighted by $|F|^2$, so wR_2 is always higher than R_1. Both R_1 and wR_2 are finite positive values and the smaller the value is, the better the refinement quality. Values of $R_1 < 5\%$ and $wR_2 < 15\%$ are typically considered good. With our instrumentation and software, and high-quality crystals, we typically reach R_1 between 2 and 5% and wR_2 between 7 and 15% (e.g., Zhang et al. 2019, 2021). When the crystal quality is less-ideal (e.g., in the case of laser heating) and the DAC opening angle is limited, the R_1 is smaller than 15% and wR_2 is smaller than 25% (e.g., Table 2). GooF takes into account the number of observed diffraction peaks and the number of fitting parameters in addition to the difference in modeled and observed scattering factors, and should approach to 1 for an ideal refinement. The GooF of the crystal structure refinement based on the diffraction data collected from our system typically ranges from 0.9 to 1.3 (e.g., Zhang et al. 2019, 2021).

Table 2 Chemical composition, lattice parameter and figures of merits of garnet and spinel samples measured at high pressure–temperature conditions using single crystal XRD

P–T condition	11.4 ± 0.5 GPa, 1450 ± 100 K	
Mineral	Garnet (almandine)	Spinel
Composition	$[Fe_{2.3}Mg_{0.7}]Al_2Si_3O_{12}$	$[Fe_{0.2}Mg_{0.8}]Al_2O_4$
Lattice parameter (Å)	11.411(8)	8.0015(14)
No. of unique peaks	82	17
Resolution (Å)	0.78	0.84
Completeness	65%	57%
R_{int}	19.03%	24.83%
R_1	6.17%	12.03%
wR_2	22.36%	20.66%
GooF	0.974	1.269

Temperature control: resistive- and laser-heating setup

There are two ways to reach high temperatures for high-pressure SXD at PX2. The first approach is to use resistive-heated DAC (Fig. 3). We typically use BX-90 type DAC to carry out resistive-heating experiment, where the samples are heated with a miniature Pt-wire heater with an internal resistance of ~ 1 Ω (Kantor et al. 2012). The heater is powered by an XHR33-33 (Sorensen) 1000 W DC power supply whose maximum output voltage and current are 33 V and 33 Å, respectively. A K- or R-type thermocouple with 0.005″ diameter is placed close to the diamond culet to read the temperature of the sample chamber. The heater, the thermocouple and the DAC are electrically insulated by high-temperature ceramics and cement. A water-cooled sample holder is used to stabilize the sample during heating. For resistive-heated DAC, the control of the sample pressure is achieved by a membrane remote pressure control system (Sect. 2.3). Resistive-heated DAC has been routinely used in high P–T single crystal diffraction experiments at PX2 (e.g., Li et al. 2021; Xu et al. 2020; Xu et al. 2018; Ye et al. 2021).

The other approach to carry out high P–T SXD experiment is through laser-heated DAC. The laser heating is achieved through a compact optical table (Fig. 4), which contains a 12 × zoom camera system (Navitar), one 532-nm

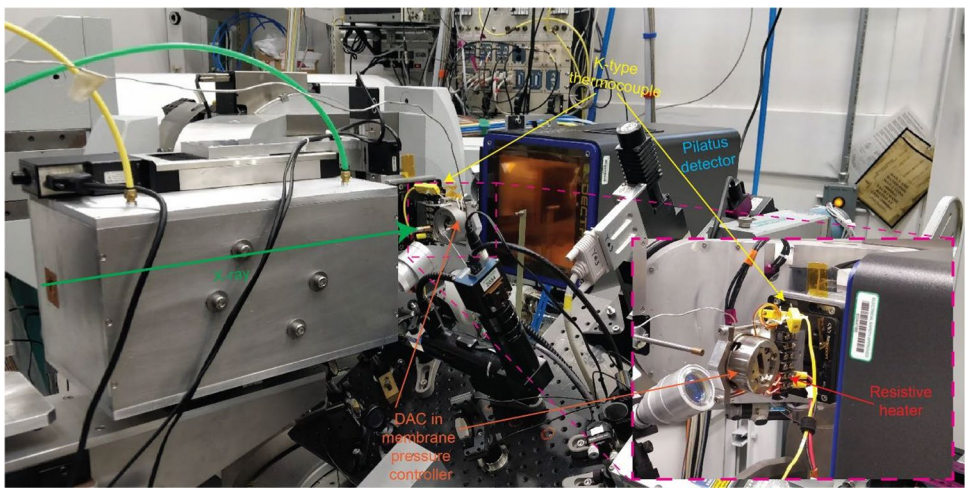

Fig. 3 Resistive-heated DAC for high P–T single crystal diffraction at PX2

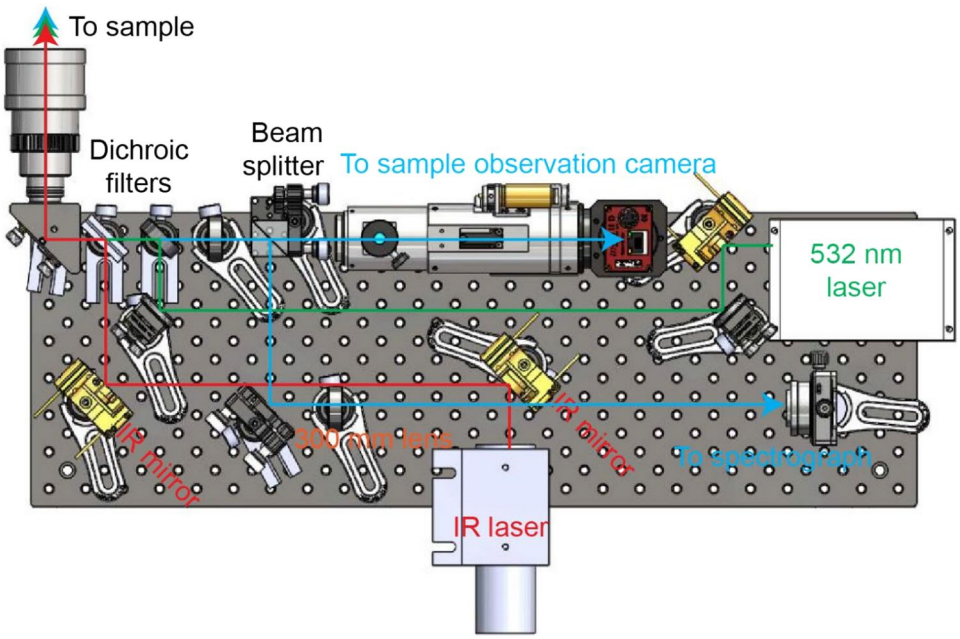

Fig. 4 Optical layout of the compact multifunctional optical table at PX2

1 W solid-state laser (LaserQuantum), one 1064-nm 200 W CW fiber laser (IPG), and a fiber-coupled spectrograph (Teledyne). The compact optical table has the following functions: (1) sample observation; (2) ruby fluorescence pressure determination; and (3) laser heating. The observation optical path is coincident with the 532-nm and 1064-nm lasers through a specially designed 80 mm working distance high-power achromat lens (geoHeat), and the laser beam position is adjusted remotely through motorized mirror mounts (Newport). The laser's focal spot size is ~ 30 μm in diameter (FWHM), slightly larger than the X-ray focus size so as to reduce the temperature gradient on the X-ray probed region.

For the LH-DAC setup, the 1064-nm IR laser is reflected by an X-ray translucent 0.5 mm thick Si mirror coated with Ag so that the IR laser is coaxial to the X-ray before hitting the sample. Round-table diamond is required in order to carry out laser-heated single-crystal diffraction experiments (Dubrovinsky et al. 2017), which requires the rotation of the DAC to reach the Bragg diffraction condition. The round table diamond keeps the laser beam continuously hitting the sample in the DAC while rotating so that the laser light will not scatter to arbitrary directions. The DAC is placed in a way that one round table diamond is facing the X-ray upstream direction, which is also the direction of laser heating. Only one side of the sample is heated by the laser.

Auxiliary instruments

For the SXD experiments at simultaneous high P–T conditions at PX2, researchers have been relying on the membrane-based remote pressure control system to control the pressure (Kantor et al. 2012). The system uses a cylinder of compressed helium gas (up to 2200 psi in pressure) and an automatic PACE5000 pressure regulator (GE) to expand/shrink a membrane diaphragm (DACtools), which exerts force on the piston/cylinder of the DAC, and hence control the pressure of the sample chamber. The pressure in the sample chamber is controlled by the gas pressure, the diamond culet size, and the friction between the piston and cylinder. For a typical diamond culet size of 300 μm, we usually reach ~ 60 GPa in the sample chamber at a gas pressure of 400–600 psi. The PACE5000 pressure regulator controls the gas pressure at a resolution of 0.01 psi. The DAC holder for the membrane system has an opening angle of ± 45°, which grants the maximum opening angle for most DACs in the SXD experiment.

Example: laser-heated single-crystal diffraction of garnet and spinel at the mantle P–T condition

We have carried out single-crystal X-ray diffraction on almandine garnet ($[Fe_{2.3}Mg_{0.7}]Al_2Si_3O_{12}$) and spinel ($[Fe_{0.2}Mg_{0.8}]Al_2O_4$) in a laser-heated diamond anvil cell at PX2. Both garnet and spinel are common rock-forming minerals with cubic crystal structure, which makes them good examples to demonstrate the capability of our system. Both crystals are synthesized from oxides in a large-volume press. The DAC is prepared using a round-table diamond and a Boehler–Almax type diamond (Boehler and De Hantsetters 2004; Dubrovinsky et al. 2017). Two Boehler–Almax designed 70° opening WC seats and a BX-90 type diamond cell are used. The culet diameter of the diamonds is 300 μm.

A Re gasket is pre-indented to 70 μm thickness, and a 200-μm diameter hole is drilled at the center of the gasket to form the sample chamber. The DAC is gas-loaded with Ne as the pressure medium (Rivers et al. 2008), which also serves as the thermal insulator to separate the sample from the diamond culets. The garnet and spinel crystals are placed in contact with each other at the center of the sample chamber, and two ruby spheres are placed close to the sample to serve as the pressure marker (Fig. 5). The SXD data are processed by APEX software (Fig. 6). About 5 W of total laser power was used to heat the sample. Under the extreme temperature gradient of laser heating, the garnet and spinel crystals broke into multiple grains during the SXD measurement. We were able to select the garnet and spinel grains with the most complete diffraction dataset and carry out crystal structure solution and refinement (Table 2). The structure refinement gave reasonable figures of merit, indicating a good diffraction data quality.

The accurate determination of the pressure and temperature is critical to simulate the mantle condition for our measurements. Due to the existence of thermal pressure, the temperature and pressure are coupled, and one cannot use a single thermal equation of state to determine both the pressure and the temperature simultaneously (Angel 2000; Angel et al. 2017). Conventional laser-heated DAC experiments usually use the thermal equation of state of external pressure markers (e.g., Au, Fei et al. 2007) and optical pyrometry (e.g., black body radiation, Prakapenka et al. 2008; Shen et al. 2005) to determine the pressure and temperature. However, the external pressure markers hinder the single-crystal diffraction measurements, as the powder diffraction rings from the pressure marker would interfere with many diffraction peaks for the sample, so one cannot introduce external

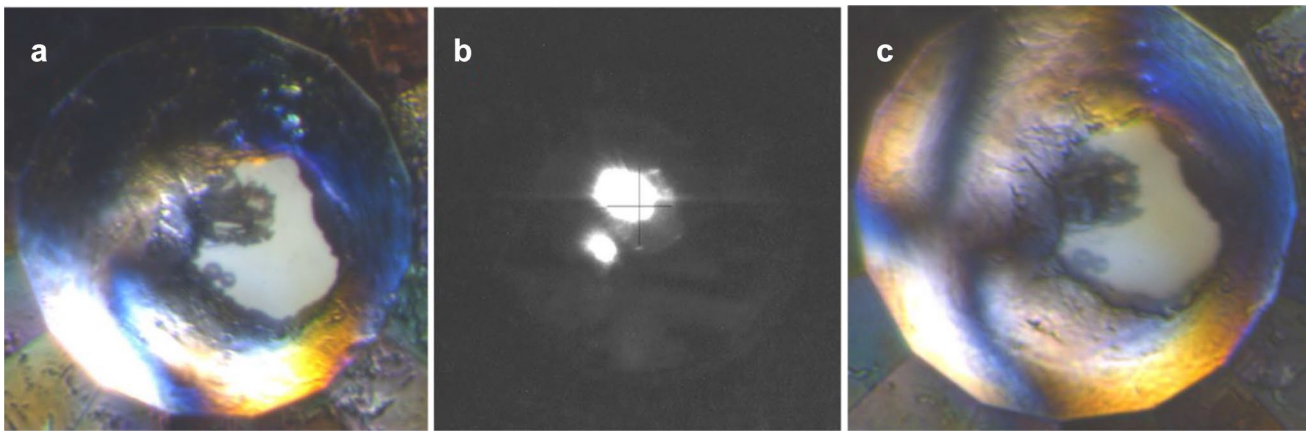

Fig. 5 Sample chamber of the pilot experiment before (**a**), during (**b**) and after (**c**) the laser heating. The diameter of the diamond culet size is 300 μm. Two ruby spheres are placed in the sample chamber away from the sample for the pressure calibration

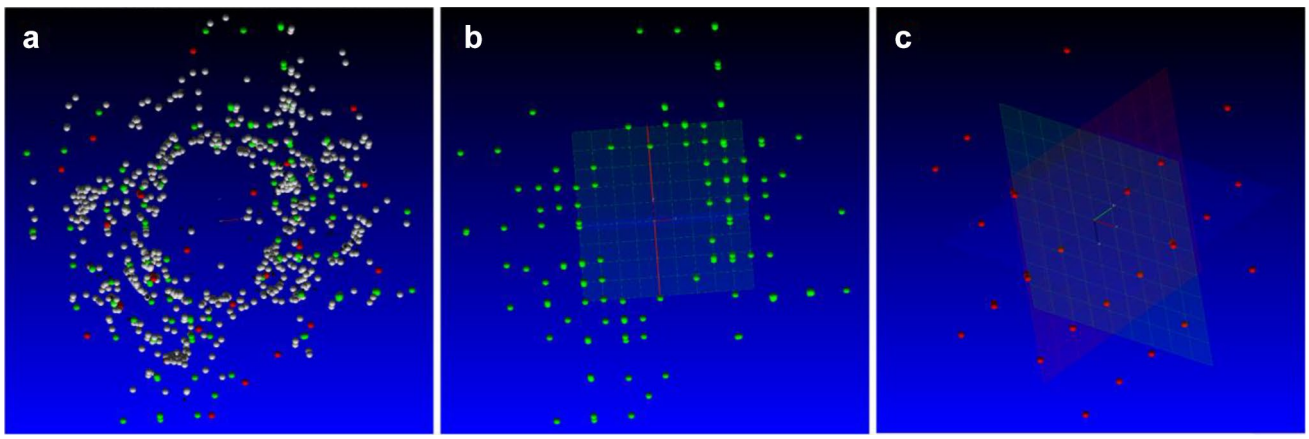

Fig. 6 **a** Distribution of diffraction peaks of the almandine + spinel sample during heating shown in Bruker APEX software. The most complete almandine (green) and spinel (red) lattices are shown in panels (**b**) and (**c**), respectively. The grey spots in panel (**a**) are from other incomplete lattices of the sample, the Ne pressure medium and the ruby pressure marker

pressure markers in single-crystal diffraction experiment. In our measurement, since the samples belong to two different minerals and the unit cell volume and chemical composition of the samples are available from the single-crystal diffraction, we are able to use the "isomeke" method and the established thermal equations of states of the two minerals to determine the pressure and the temperature simultaneously (Adams et al. 1975; Angel et al. 2017). The principle of the isomeke method is briefly explained as follows: the thermal equation of states establishes a relationship among the P–V–T of the mineral with a known composition. Once the unit cell volume ($V = V_{exp}$) is fixed, the pressure (P) and temperature (T) forms a curve in the P–T space, named the isomeke (from the Greek "equal" and "length") (Adams et al. 1975; Angel et al. 2017). When the isomekes of the two samples cross in the P–T space, the pressure and temperature are determined simultaneously at the crossing. We expect that the precision and accuracy of the isomeke approach will be comparable with the conventional method, as the sample geometries of the two approaches are similar (two crystals in close contact, just like the external pressure markers in close contact with the sample in the conventional approach).

We have tested our isomeke approach in the laser-heated SXD experiment between garnet and spinel. The isomekes were computed using the following equations:

$$P = \frac{3K_{T0}}{2}\left[\left(\frac{V_{T0}}{V_{exp}}\right)^{\frac{7}{3}} - \left(\frac{V_{T0}}{V_{exp}}\right)^{\frac{5}{3}}\right]\left\{1 + \frac{3}{4}\left(K'_{T0} - 4\right)\left[\left(\frac{V_{T0}}{V_{exp}}\right)^{\frac{2}{3}} - 1\right]\right\}$$

$$K_{T0} = K_0 + \left(\partial K_T/\partial T\right)_P (T - 300)$$

$$V_{T0} = V_0 \exp \int_{300}^{T} \alpha_T \mathrm{d}T$$

$$\alpha_T = \alpha_0 + \alpha_1 T$$

We used published thermoelastic parameters to calculate the isomekes. For garnet, $V_{T0} = 1527.0$ Å^3, $K_0 = 171.85$ GPa, $K'_{T0} = 5.49$, $\left(\partial K_T/\partial T\right)_P = -0.0334$ GPa/K, $\alpha_0 = 1.79 \times 10^{-5}$ K^{-1}, and $\alpha_1 = 2.26 \times 10^{-8}$ K^{-2} (Xu et al. 2019). For spinel, $V_{T0} = 530.5$ Å^3, $K_0 = 197.2$ GPa, $K'_{T0} = 4.4$, $\left(\partial K_T/\partial T\right)_P = -0.023$ GPa/K, $\alpha_0 = 2.03 \times 10^{-5}$ K^{-1}, and $\alpha_1 = 5.4 \times 10^{-9}$ K^{-2} (Fan et al. 2008). Both sets of thermoelastic parameters were determined by resistive-heated DAC experiments. Using the V_{exp} determined by our in-situ laser heating experiment ($V_{exp\text{-}garnet} = 1485.7$ Å^3, $V_{exp\text{-}spinel} = 512.3$ Å^3, Table 2), the two isomekes cross at 1450 K and 11.4 GPa (Fig. 7). In order to validate our

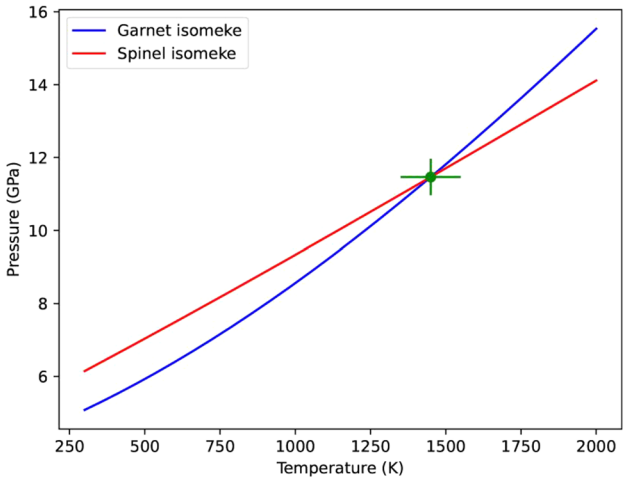

Fig. 7 Pressure and temperature calculation of the laser-heated single crystal diffraction experiment using the isomekes of garnet and spinel. Green symbol indicates the cross section of the two isomekes (11.4 GPa, 1450 K) and their corresponding uncertainties (±0.5 GPa, ± 100 K)

temperature measurement and check the temperature gradient within the DAC, we took the same DAC to GSECARS beamline 13-ID-D, heated the sample from one side with the same laser power as the partitioning experiment, and measured the temperatures from both sides using the optical pyrometry system in 13-ID-D (Prakapenka et al. 2008). The black body radiation gave the temperature of the heating side as 1486 ± 3 K and the temperature of the non-heating side as 1398 ± 9 K (Fig. 8). The average temperature was 1442 K, consistent with the estimations from the isomeke approach (1450 K). We found that there is a temperature gradient of ~ 100 K between the heating side and the non-heating side, and we propose to use 100 K as the uncertainty of the error. The pressure uncertainty is estimated at 0.5 GPa, based on the average P–T gradient of the isomeke (0.005 GPa/K). Though we could not validate the sample's pressure in-situ while heating as we did not have external pressure marker near the sample, the sample chamber's pressure was determined as 8 GPa using ruby fluorescence while not heating (Dewaele et al. 2008). The thermal pressure of the sample during heating is estimated as 3.4 GPa, which is in the same magnitude for published laser-heating experiments (Zhang et al. 2016b).

Conclusion and outlook

The high-pressure SXD technique is becoming more and more popular in the Earth, planetary and material sciences. At PX2, the high-pressure SXD experiments have been carried out to study phase transitions, structure identification, chemical compositions, thermoelasticity, and synthesis of

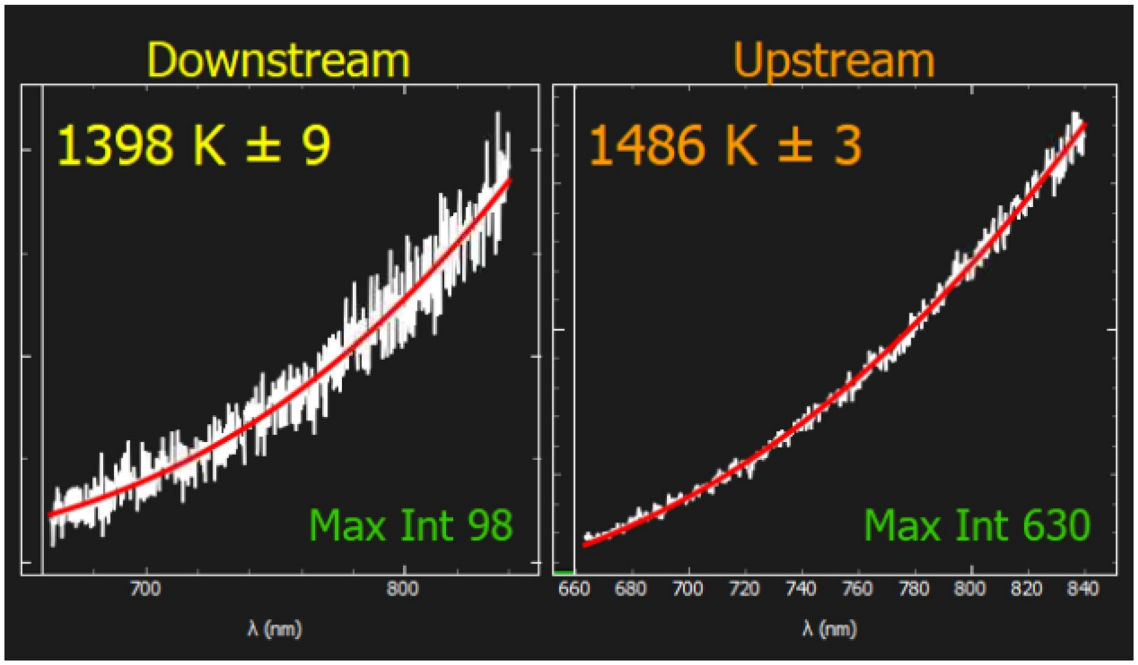

Fig. 8 Black-body radiation fitting of the temperature of the same sample measured in GSECARS 13-ID-D with the identical heating setup (same laser power, heating only from the upstream side)

novel materials. The samples studied at PX2 have covered crust, mantle and core minerals within and beyond the earth, and materials that have potentially significant impacts on our environment. As a user facility open to the earth, planetary and environmental research communities, we expect to continue our momentum and keep delivering state-of-the-art SXD experimental capabilities to our communities.

For future developments, we intend to focus on the following aspects, so as to expand the P–T range for SXD measurements, as well as improve the diffraction data quality and resolution.

(A) Optimized X-ray instrument: For SXD experiments, the larger the X-ray energy, the shorter the X-ray wavelength, and the more reciprocal space the X-ray will probe. High energy X-ray will provide more information about the mineral crystal structure and chemical composition as well as a better data quality. Currently, at PX2 we are using a Si(311) single crystal monochromator, which provides X-rays at 28.6 keV at the scattering angle in use. We plan to upgrade the monochromator crystal to Si(400), which will provide 34.5 keV X-rays at the same scattering angle. Increasing energy from 28.6 to 34.5 keV will decrease the X-ray wavelength from 0.434 to 0.359 Å. Given the same DAC opening angle design, upgrading the monochromator crystal would increase the reciprocal space probing range by 76% as it is proportional to the cube of the wavenumber of the incident X-ray ($[0.434/0.359]^3 - 1 = 76\%$), which is expected to improve the resolution of the single crystal diffraction data by ~ 20%. The current focusing mirror and the X-ray area detector can still be used, although replacing the detector with one that has a CdTe-based sensor will improve its quantum efficiency at 34.5 keV.

(B) Optimized optical instrument: We plan to upgrade the current laser-heating SXD setup from one side heating to double-sided heating so as to reduce the axial temperature gradient and increase the heating power. The proposed double-sided laser-heated SXD setup not only provides a reliable way to analyze the chemical composition of mantle minerals, but also opens the opportunity to synthesize/characterize new materials at pressures between 10 and 100 GPa and temperatures between 1000 and 4000 K, which covers the P–T condition of most part of the earth's mantle (1–135 GPa, 1000–4000 K, Mao and Hemley 2007). We expect to synthesize the previously-unexplored core and mantle phases with this setup and study their crystal structures. The most prominent challenge for such high P–T synthesis is that it involves the optimization of pressure, temperature and sample composition, and finding the most efficient synthesis routine could be time-consuming. The advantage of our laser-heated high pressure system is that it combines both the sample synthesis apparatus with the sample characterization

facility, so that one can monitor the sample synthesis in-situ, which will significantly improve the efficiency in finding the most effective synthesis routine. We will improve temperature measurements by introducing optical pyrometry based on grey-body radiation, and we will upgrade the spectrometer and its camera accordingly to be compatible with the optical pyrometry approach.

Acknowledgements This work was performed at GeoSoilEnviroCARS (Sector 13), Partnership for Extreme Crystallography program (PX2), Advanced Photon Source (APS), and Argonne National Laboratory. GeoSoilEnviroCARS is supported by the National Science Foundation-Earth Sciences (EAR-1634415) and Department of Energy-Geosciences (DE-FG02-94ER14466). PX2 program is supported by COMPRES under NSF Cooperative Agreement EAR-1661511. Use of the Advanced Photon Source was supported by the U.S. Department of Energy, Office of Science, Office of Basic Energy Sciences, under Contract No. DE-C02-6CH11357.

Funding Funding was provided by Division of Earth Sciences (Grant No. EAR-1634415, EAR-1661511), U.S. Department of Energy (Grant No. DE-FG02-94ER14466) and Basic Energy Sciences (Grant No. DE-C02-6CH11357).

References

Adams HG, Cohen LH, Rosenfeld JL (1975) Solid inclusion piezothermometry. 1. Comparison dilatometry. Am Mineral 60(7–8):574–583

Angel RJ (2000) Equations of state. High-Temp High-Press Cryst Chem 41:35–59. https://doi.org/10.2138/rmg.2000.41.2

Angel RJ, Mazzucchelli ML, Alvaro M, Nestola F (2017) EosFit-Pinc: a simple GUI for host-inclusion elastic thermobarometry. Am Miner 102(9):1957–1960. https://doi.org/10.2138/am-2017-6190

Bernstein H, Hammersley A (2006) Specification of the crystallographic binary file (CBF/imgCIF). International Tables for Crystallography, pp 37–43

Boehler R, De Hantsetters K (2004) New anvil designs in diamond-cells. High Pressure Res 24(3):391–396. https://doi.org/10.1080/08957950412331323924

Dera P, Zhuravlev K, Prakapenka V, Rivers ML, Finkelstein GJ, Grubor-Urosevic O, Tschauner O, Clark SM, Downs RT (2013) High-pressure single-crystal micro- X-ray diffraction (SCμXRD) analysis with GSE_ADA/RSV software. High Pressure Res 33(3):466–484

Dewaele A, Torrent M, Loubeyre P, Mezouar M (2008) Compression curves of transition metals in the Mbar range: experiments and projector augmented-wave calculations. Phys Rev B. https://doi.org/10.1103/Physrevb.78.104102

Dubrovinsky L, Koemets E, Bykov M, Bykova E, Aprilis G, Pakhomova A, Glazyrin K, Laskin A, Prakapenka VB, Greenberg E, Dubrovinskaia N (2017) Diamond anvils with a round table designed for high pressure experiments in DAC. High Pressure Res 37(4):475–485. https://doi.org/10.1080/08957959.2017.1388802

Eng P, Newville M, Rivers M, Sutton S (1998) Dynamically figured Kirkpatrick Baez x-ray microfocusing optics. Proc SPIE 3449:145–156

Fan D, Zhou W, Liu C, Liu Y, Jiang X, Wan F, Liu J, Li X, Xie H (2008) Thermal equation of state of natural chromium spinel up to 26.8 GPa and 628 K. J Mater Sci 43(16):5546–5550. https://doi.org/10.1007/s10853-008-2825-5

Fei YW, Ricolleau A, Frank M, Mibe K, Shen GY, Prakapenka V (2007) Toward an internally consistent pressure scale. Proc Natl Acad Sci USA 104(22):9182–9186. https://doi.org/10.1073/pnas.0609013104

Hazen RM, Finger LW (1982) Comparative crystal chemistry: temperature, pressure, composition and the variation of crystal structure. Wiley, Chichester

Hu Y, Kiefer B, Bina CR, Zhang DZ, Dera PK (2017) High-pressure gamma-$CaMgSi_2O_6$: Does penta-coordinated silicon exist in the Earth's mantle? Geophys Res Lett 44(22):11340–11348. https://doi.org/10.1002/2017GL075424

Kantor I, Prakapenka V, Kantor A, Dera P, Kurnosov A, Sinogeikin S, Dubrovinskaia N, Dubrovinsky L (2012) BX90: a new diamond anvil cell design for X-ray diffraction and optical measurements. Rev Sci Instrum 83(12):125102. https://doi.org/10.1063/1.4768541

Lavina B, Dera P, Downs RT (2014) Modern X-ray diffraction methods in mineralogy and geosciences. Rev Miner Geochem 78(1):1–31. https://doi.org/10.2138/rmg.2014.78.1

Li B, Xu J, Zhang D, Ye Z, Huang S, Fan D, Zhou W, Xie H (2021) Thermoelasticity and stability of natural epidote at high pressure and high temperature: implications for water transport during cold slab subduction. Geosci Front 12(2):921–928. https://doi.org/10.1016/j.gsf.2020.05.022

Mao HK, Hemley RJ (2007) The high-pressure dimension in earth and planetary science. Proc Natl Acad Sci 104(22):9114–9115

McMahon MI (2012) High-pressure crystallography. Top Curr Chem 315:69–110

Prakapenka VB, Kubo A, Kuznetsov A, Laskin A, Shkurikhin O, Dera P, Rivers ML, Sutton SR (2008) Advanced flat top laser heating system for high pressure research at GSECARS: application to the melting behavior of germanium. High Press Res 28(3):225–235. https://doi.org/10.1080/08957950802050718

Prescher C, Prakapenka VB (2015) DIOPTAS: a program for reduction of two-dimensional X-ray diffraction data and data exploration. High Pressure Res 35(3):223–230. https://doi.org/10.1080/08957959.2015.1059835

Rivers M, Prakapenka VB, Kubo A, Pullins C, Holl CM, Jacobsen SD (2008) The COMPRES/GSECARS gas-loading system for diamond anvil cells at the advanced photon source. High Pressure Res 28(3):273–292. https://doi.org/10.1080/08957950802333593

Sheldrick GM (2008) A short history of SHELX. Acta Crystallogr A 64:112–122

Shen GY, Mao HK (2017) High-pressure studies with x-rays using diamond anvil cells. Rep Prog Phys 80(1):1–53. https://doi.org/10.1088/1361-6633/80/1/016101

Shen GY, Prakapenka VB, Eng PJ, Rivers ML, Sutton SR (2005) Facilities for high-pressure research with the diamond anvil cell at GSECARS. J Synchrotron Radiat 12:642–649. https://doi.org/10.1107/S0909049505022442

Stixrude L, Lithgow-Bertelloni C (2005) Thermodynamics of mantle minerals—I. Physical properties. Geophys J Int 162:610–632

Xu W, Lithgow-Bertelloni C, Stixrude L, Ritsema J (2008) The effect of bulk composition and temperature on mantle seismic structure. Earth Planet Sci Lett 275:70–79

Xu JG, Zhang DZ, Fan DW, Zhang JS, Hu Y, Guo XZ, Dera P, Zhou WG (2018) Phase transitions in orthoenstatite and subduction zone dynamics: effects of water and transition metal ions. J Geophys Res Solid Earth 123(4):2723–2737. https://doi.org/10.1002/2017JB015169

Xu J, Zhang D, Fan D, Dera PK, Shi F, Zhou W (2019) Thermoelastic properties of eclogitic garnets and omphacites: implications for deep subduction of oceanic crust and density anomalies in the upper mantle. Geophys Res Lett 46(1):179–188. https://doi.org/10.1029/2018GL081170

Xu JG, Fan DW, Zhang DZ, Guo XZ, Zhou WG, Dera PK (2020) Phase transition of enstatite–ferrosilite solid solutions at high pressure and high temperature: constraints on metastable orthopyroxene in cold subduction. Geophys Res Lett. https://doi.org/10.1029/2020GL087363

Ye Z, Fan D, Tang Q, Xu J, Zhang D, Zhou W (2021) Constraining the density evolution during destruction of the lithospheric mantle in the eastern North China Craton. Gondwana Res 91:18–30. https://doi.org/10.1016/j.gr.2020.12.001

Yong T, Dera P, Zhang D (2019) Single-crystal X-ray diffraction of grunerite up to 25.6 GPa: a new high-pressure clinoamphibole polymorph. Phys Chem Miner 46(3):215–227. https://doi.org/10.1007/s00269-018-0999-1

Zhang DZ, Hu Y, Dera PK (2016a) Compressional behavior of omphacite to 47 GPa. Phys Chem Miner 43(10):707–715. https://doi.org/10.1007/s00269-016-0827-4

Zhang DZ, Jackson JM, Zhao JY, Sturhahn W, Alp EE, Hu MY, Toellner TS, Murphy CA, Prakapenka VB (2016b) Temperature of Earth's core constrained from melting of Fe and $Fe_{0.9}Ni_{0.1}$ at high pressures. Earth Planet Sci Lett 447:72–83. https://doi.org/10.1016/j.epsl.2016.04.026

Zhang DZ, Dera PK, Eng PJ, Stubbs JE, Zhang JS, Prakapenka VB, Rivers ML (2017) High pressure single crystal diffraction at PX2. Jove-J Vis Exp. https://doi.org/10.3791/54660

Zhang DZ, Hu Y, Xu J, Downs RT, Hammer JE, Dera PK (2019) High-pressure behavior of liebenbergite: The most incompressible olivine-structured silicate. Am Miner 104(4):580–587. https://doi.org/10.2138/am-2019-6680

Zhang DZ, Chen M, Dera PK, Eng PJ (2021) Experimental calibration of the reduced partition function ratios of tetrahedrally coordinated silicon from the Debye–Waller factors. Contrib Miner Petrol 176(9). https://doi.org/10.1007/s00410-021-01820-6